

Structure of ice multilayers on metals

H. Witek and V. Buch

Citation: *The Journal of Chemical Physics* **110**, 3168 (1999); doi: 10.1063/1.477912

View online: <http://dx.doi.org/10.1063/1.477912>

View Table of Contents: <http://aip.scitation.org/toc/jcp/110/6>

Published by the [American Institute of Physics](#)

COMPLETELY

REDESIGNED!



**PHYSICS
TODAY**

Physics Today Buyer's Guide
Search with a purpose.

Structure of ice multilayers on metals

H. Witek and V. Buch

Department of Physical Chemistry and the Fritz Haber Research Center, The Hebrew University, Jerusalem 91904, Israel

(Received 28 July 1998; accepted 2 November 1998)

Simulations are presented of model ice adsorbate layers on metals, in the coverage range of 2–4 bilayers. The issues investigated include the decay mechanism of ferroelectricity imposed by bonding of the first bilayer to the metal, and the influence of first bilayer flattening (due to bonding to the metal) on the adsorbate structure. A new kind of defect in the ice structure—an internal dangling OH bond—is reported, and shown to provide a mechanism for decay of ferroelectricity over the range of 2–3 bilayers only. Flattening of the bottom bilayer results in “sandwich-like” adsorbate structures, and disappearance of most of dangling-OH bonds from the upper surface.

© 1999 American Institute of Physics. [S0021-9606(99)70106-6]

I. INTRODUCTION

Recently, new and exciting experimental data are becoming increasingly available on molecular properties of ice multilayers on metals, e.g., Refs. 1–9. Here, nondissociative adsorption of H₂O on metal surfaces is considered. Specifically, the objective is to use computer simulations in order to advance the understanding of thin ice layer structure on metals, in the thickness range of 2–4 bilayers. It is well known that ice surfaces display physical behaviors quite distinct from bulk ice; e.g., the surface melting point is well below that of the bulk.¹⁰ The ordinary hexagonal ice Ih is composed of stacked buckled hexagonal bilayers,¹⁰ and corresponds to a nearly perfect tetrahedral network of hydrogen bonds. This structure is favorable to the interior, but not to the surface. This is since surface formation is associated with numerous “dangling” H and O atoms with unsaturated hydrogen bond coordination. Several studies suggested relaxation of ice surfaces which is associated with increase in the number of hydrogen bonds, and concurrent loss of translational order.^{11,12} In the present study, related surface relaxation phenomena are discussed for thin ice layers.

Some metal surfaces provide binding sites approximately matching the O-atom arrangement in hexagonal layers of ice Ih (Ref. 13, and references therein). Adsorption of H₂O on such surfaces has been extensively investigated. Here we focus specifically nondissociative adsorption. (There are systems, in which water dissociates and forms oxide or hydroxide layers between the metal and the ice layer.) Recently, experimental measurements have been carried out of He scattering from ordered layers of ice on Pt(111)³ and Rh(111),⁴ indicating lateral arrangement of water O atoms that matches the (0001) surface of ice Ih. These and other results suggest formation of ordinary ice layers already at a bilayer coverage.^{3,4,13–15} But this view raises a number of questions. First, there is a question of a vertical arrangement of the first bilayer H₂O above the metal surface. If an ordinary buckled ice bilayer is assumed,^{13,15} the perpendicular to the surface coordinate of the “top” O atoms is nearly 1 Å larger than that of the bottom atoms; thus, the

water–surface interaction of the upper layer should be substantially reduced with respect to that of the lower layer. It has been shown in fact that a single D₂O bilayer on Ru(001) is flattened, presumably due to the attraction of the upper half of the bilayer to the metal surface.¹³ We shall show that such flattening affects dramatically the hydrogen bond network in the following bilayers. However the lateral unit cell vectors on the Ru(001) surface are larger than those of ice, which may be a contributing factor to the flattening. The flattening may be reduced or absent on surfaces such as Rh(111), for which the mismatch with the lateral unit cell dimensions of ice is much smaller.⁴ Thus, the first issue to be addressed is the influence of the vertical arrangement of the first bilayer on the bonding structure of the following bilayers.

The second issue pertains to the arrangement of the H atoms in thin ice layers on metals, which has been a subject of considerable discussion. H-atom arrangement within the ordinary ice Ih is first reviewed.¹⁰ Ice Ih is proton disordered. That is, while O atoms form a periodic pattern, the H atoms are arranged at random within the constraints of the so-called ice rules—two chemically bonded and two hydrogen bonded H atoms around each O atom. Thus, a H atom on each nearest-neighbor O–O axis can occupy one of the two possible sites, near each of the O atoms. The resulting global dipole of ice Ih is zero. In the presence of KOH impurity, partial proton ordering can be induced in ice at 72 K;¹⁶ the proton ordered ice structure was recently identified¹⁷ as ferroelectric Cmc2₁.

The question is the H atom arrangement in thin ice layers on metals. Metal bonding of water via O atoms was suggested to enforce ferroelectric ordering along the *c* axis^{13,15} (see Fig. 1). That is, there may be proton disorder within the first bilayer, but all H atoms along the *c* axis are believed to point up. It is important to realize, that in an ideal defectless ice structure, the ferroelectric ordering of the first bilayer along the *c* axis should propagate indefinitely to the upper layers. This is quite different, for example, from the case of a magnetic analog. Polarization of a layer of spins on the surface of a magnet which is above its Curie temperature will

2 bi-layers, ferro., before relaxation

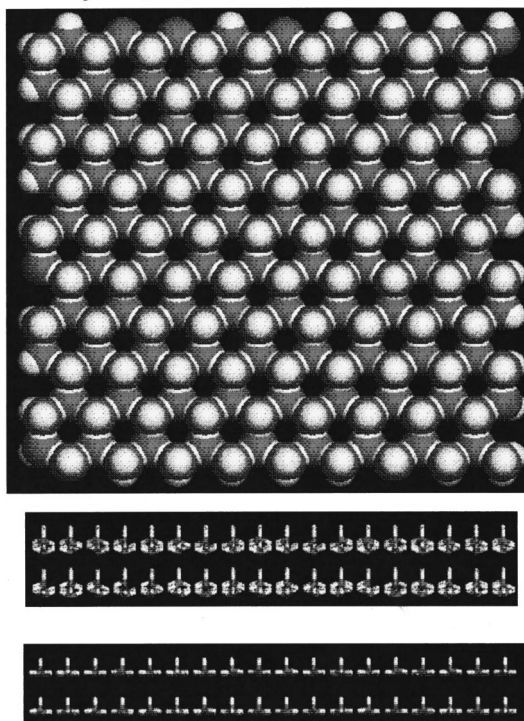


FIG. 1. A two bilayer ferroelectric model before relaxation took place, top, and side view. The two side views correspond to the FLAT (bottom) and PUCKERED models, respectively.

certainly not result in magnetization of the whole sample; the magnetization will decay over the magnetic coherence length. However, in contrast to the spins, the water molecules are constrained by the tetrahedral hydrogen bond network. Ferroelectric ordering along the c axis cannot be disrupted without disrupting the bond network, that is, without creating defects. One can confirm that by inspection of 3D ice models—there is no way to flip the direction of some of the OH bonds along the c axis without breaking any hydrogen bonds.

A recent optical sum-frequency study² in fact suggested ferroelectric ordering with decay length of ~ 15 bilayers, near 130 K. But that would imply an ice surface covered by a layer of repulsing, approximately parallel dipoles (dangling OH bonds, see Fig. 1), and ferroelectricity at temperature nearly twice higher than that of the proton order-disorder transition temperature in ordinary ice. In Ref. 5, the question has been raised on the absolute amount of ordering, i.e., what is the fraction of oriented molecules in the sample. It has been argued that extensive ferroelectric ordering over substantial thickness should be reflected by a very large work function value, contrary to current experimental evidence.^{5,9,18}

Complete modeling of ice layers on metals requires knowledge of water-water and water-metal interactions; moreover water-water interactions may be modified by the metal. Our objective at this stage is more modest. To avoid dealing with metal-water interaction, the structure of the first bilayer was adopted from past suggestions based on analyses of experimental data,^{13,15} and kept fixed throughout

the simulations; and the structure of further bilayers was investigated, given this first (rigid) bilayer structure. The calculation employed a polarizable water-water potential,¹⁹ and was double checked with TIP4P.²⁰ However, the interaction of the second and higher bilayers with the metal was neglected (except for some runs including image charges). This scheme is of course approximate and we anticipate further investigations including detailed interaction with the metal. Studies of this kind have been used recently to study H₂O freezing between metal plates,²¹ and liquid-metal interfaces.²²

Section II describes the computational procedures. The results are discussed in Sec. III and summarized in Sec. IV.

II. COMPUTATIONAL PROCEDURE

A. The models of the bottom (rigid) H₂O bilayer

The first structure, denoted FLAT, was adopted from a low energy electron diffraction (LEED) study of a H₂O bilayer on Ru(001).¹³ Of course, it is not clear that upon deposition of the second bilayer, the structure of the first one is preserved; however, this structure is convenient for investigating possible effects of the first bilayer flattening on the subsequent bilayers. The nearest-neighbor lateral O-O distance is 2.71 Å, and the vertical distance between O atoms in the two layers of a bilayer is only 0.1 Å. Reference 13 does not provide H-atom locations, except for the suggestion that dangling H atoms in the top half of the bilayer point up. This suggestion was adopted. The H atoms within the bilayer were placed at random, within the ice rules, on the nearest-neighbor O-O axes. Finally, the HOH angles were reset to 104.52° in accord with the simulation potential used (for this purpose, the H-atom positions in each molecule were corrected by equal but opposite vectors). Comment: in this model, the bilayer is nearly flattened into a single layer. It will still be denoted a ‘bilayer’ for the sake of consistency.

The second structure used to model the bottom ice bilayer was an ideal puckered hexagonal (0001) bilayer of ice, with all OH bonds along the c axis pointing up. This structure, denoted PUCKERED, may be the correct one on Rh(111) (whose lateral unit vectors match well those of ice⁴), and on Pt(111) (for which lateral unit vectors matching ice were obtained experimentally, despite the mismatch with the underlying metal^{3,14}). As in the FLAT model, proton disorder was assumed within the bilayer. Nearest-neighbor O-O distance was set to 2.74 Å.

Finally, a few simulations were carried out with an intermediate structure SEMI, in which the vertical distance between O atoms in the bilayer was reduced to 0.5 Å with respect to PUCKERED.

B. The initial structures of the following bilayers

The initial position of the following bilayers were chosen in several ways. In most cases, the generation procedure of upper bilayers was the same as the first one, but in some calculations (denoted below as SANDWICH), some of the bilayers were inverted. That is, a bilayer was replaced by its mirror image (the mirror was the xy plane), having the same mean z value for the O atoms as the original bilayer. (The

TABLE I. Summary of the different simulations runs of ice layers. SAND and FERRO denote, respectively, a sandwich and a ferroelectric *initial* structure, note that structural changes occur during the simulation.

Layers	Model	t (ps) ^a	$\bar{E}^b(T^\circ)$	\bar{E}^d	M_z^c	$H(\text{dang})^f$	$H(\text{dang, out})^g$
2	FLAT/FERRO	10	-10.43 (111 K)	-10.73 (9 K)	0.56	13	13
2	FLAT/SAND	10	-10.54 (120 K)	-10.83 (10 K)	0.40	0	0
3	FLAT/FERRO	10	-10.57 (114 K)	-11.03 (12 K)	0.54	52	19
4	FLAT/FERRO	10	-11.14 (119 K)	-11.67 (11 K)	0.48	3	0
4	FLAT/SAND ^h	10	-11.12 (103 K)	-11.64 (11 K)	0.47	1	0
2	SEMI/FERRO	10	-9.80 (99 K)	-10.09 (10 K)	0.63	23	8
2	PUCKD/FERRO	30	-9.71 (32 K)	-9.71 (32 K)	1.87	90	90
2	PUCKD/SAND	40	-10.03 (32 K)	-10.03 (32 K)	0.85	95	10
2	PUCKD/FERRO ⁱ	190	-9.69 (142 K)	-10.20 (12 K)	1.17	96	36
2	PUCKD/SAND	10	-9.83 (98 K)	-10.10 (13 K)	0.88	91	6
3	PUCKD/FERRO ^j	178	-10.50 (133 K)	-11.14 (13 K)	1.67	97	42

^aLength of a simulation.

^bMean potential energy per molecule, in kcal/mol, during the simulation.

^cMean temperature of a simulation.

^dMean potential energy per molecule, in kcal/mol, in the final configuration, usually after recooling near 10 K. The final temperature is given in brackets.

^e $M_z = \sum \bar{\mu}_z$, where $\bar{\mu}_z$ is a mean molecular dipole in a bilayer, in the direction perpendicular to the surface, and the sum is over all bilayers. Debye units.

^fNumber of dangling hydrogens in the final configuration, after cooling; cutoff of 2.3 Å was used for the O–H distance, to define a hydrogen bond.

^gNumber of “bare” dangling H atoms, pointing into the vacuum from the upper surface; in an initial unrelaxed ferroelectric model this number is 90. Sometimes several molecules move out to the top of the last layer in the course of the simulation; their dangling bonds are not included in the count.

^hA simulation initiated in a double sandwich configuration, with sandwiches shifted with respect to each other.

ⁱA 170 ps simulation was run during which the temperature increased from 100 to 155 K due to structural relaxation. The final structure of this run was recooled near 100 K; the temperature remained stable for another 20 ps of the simulation.

^jHeating from 100 to 140 K occurred during the simulation.

mean z of the bilayer was then “jiggled” up and down to find an approximate minimum energy with respect to z , the resulting z shift was about 0.2 Å.) This procedure was used for a two bilayer sandwich. For a four bilayer sandwich, the second sandwich was generated by replicating the first one.

In all models, each ice bilayer included 180 water molecules. Two-dimensional periodic boundary conditions were employed in all simulations.

C. The potential

The calculation employed a modified version of an empirical polarizable water potential proposed in Ref. 23. The modification of the potential was recently carried out,¹⁹ in an effort to provide a balanced description of all water phases (solid, liquid, and clusters), and in particular to make the observed ordered ferroelectric form of ice energetically favorable with respect to proton-disordered ice.¹⁷ The parameters modified with respect to the original version²³ are $r_s = 1.25$ Å, $b_\infty = 2.65$ a.u.; moreover the polarizability center was shifted down the bisector of H₂O, 0.48 Å from O towards the H atoms (the latter shift stabilizes the ferroelectric Cmc2₁ form of ice with respect to disordered ice). While we report here the results obtained for this potential only, additional simulations were carried out with TIP4P,²⁰ with and without image charges in the metal. Several additional simulations were carried out for the two bilayer case, with the polarizable potential, while only including images of perma-

nent charges. The results of all the additional simulations were qualitatively consistent with the ones reported below.

D. Details of the classical trajectory simulations

As noted above, the bottom bilayer, which is attached to the metal, was assumed rigid. Classical trajectory simulations were carried out on water molecules in the upper bilayers. We report here results for 2–4 bilayers (the numbers include the bottom rigid bilayer). The objective is to study the structure adopted by the upper bilayers, for a given bottom bilayer model. The relaxation cycle included heating of the initial structure to ~110 K, a classical trajectory near 110 K, and recooling to ~10 K. A classical trajectory was run for a period between 10 and 190 ps (see Table I). The temperature near 110 K was selected, since a number of relevant experimental studies pertain to this temperature region. During the course of the simulation, the temperature of some of the models increased by as much as ~50 K, due to structural relaxation. The model was recooled in the end of the simulation, in an effort to assess the ground state structure.

The cooling and the heating protocols employed a sequence of steps, consisting of rescaling of molecular velocities (equivalent to 20 K temperature jumps), followed by 1 ps simulation runs; the steps were repeated until the desired temperature was achieved. Potential cutoff of 10 Å was used. The correction for the resulting lack of energy conservation was carried out every 0.1 ps, by rescaling the velocities. A time step of 40 a.u.=0.968 fs was used. The water molecules

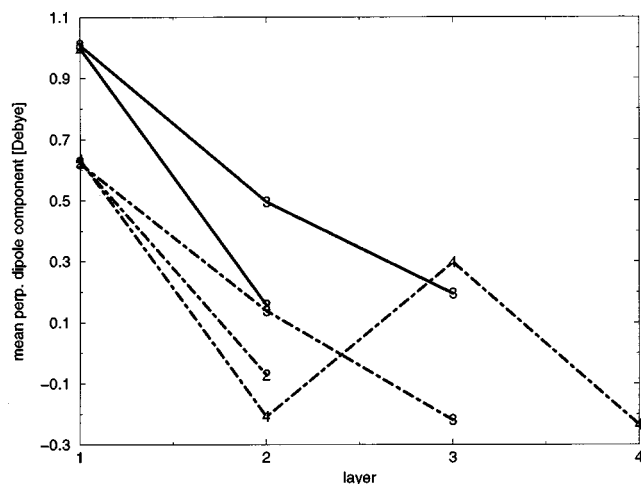


FIG. 2. $\bar{\mu}_z$, the mean z component of the molecular dipole in a bilayer, as a function of the bilayer index. Dotted-dashed—the FLAT model, solid—PUCKERED. The number of bilayers in the model is marked on each respective plot. The results are for the end of the trajectory, before the recoiling.

were assumed rigid, the SHAKE/Verlet algorithm was used to enforce the rigidity.²⁴ To converge induced dipoles in calculations of forces and energies, nine iterations were employed.

A comment should be made on the use of a simple potential cutoff in the simulations. In studies of condensed phase systems made of molecules with large dipoles, treatment of long range forces may require particular attention in calculations of some of the properties.^{19(a),25} The problem is that the dipole-dipole interaction decays as r^{-3} , while in a three-dimensional system the number of dipoles at a distance between r and $r + dr$ increases as r^2 ; thus the effective decay rate of the interaction is very slow (r^{-1}). However this difficulty is less serious in the case of a two-dimensional system such as adsorbate on surface, since the number of dipoles increases with distance only as r^1 , and therefore the interaction decays, effectively, as r^{-2} . We already used quite successfully a simple cutoff in the treatment of adsorbate-surface problems dominated by dipole-dipole interactions.²⁶ We expect its use to be reasonable in the present system as well, especially considering that the important effects are due to short range interactions (such as molecular rearrangements that increase the number of hydrogen bonds, see below). A more refined calculations of the system energetics will require, of course, a better treatment of long range forces, such as the Ewald summation.

The results are summarized in Table I, and in the figures. Two of the calculated quantities are related to the experimental work function. The quantity plotted in Fig. 2, $\bar{\mu}_z$, is the mean molecular dipole in a bilayer, in the direction perpendicular to the surface. The contribution of a bilayer to the work function is expected to be proportional⁵ to $\bar{\mu}_z$ (except for the first bilayer, for which direct interaction with the metal is of importance). The quantity M_z given in Table I, referred to below as “total dipole,” is the sum over $\bar{\mu}_z$ values of all the bilayers. The PUCKERED results in Figs. 2 and 3 pertain to the longest PUCKERED/FERRO trajectories in Table I, the FLAT results—to FLAT/FERRO.

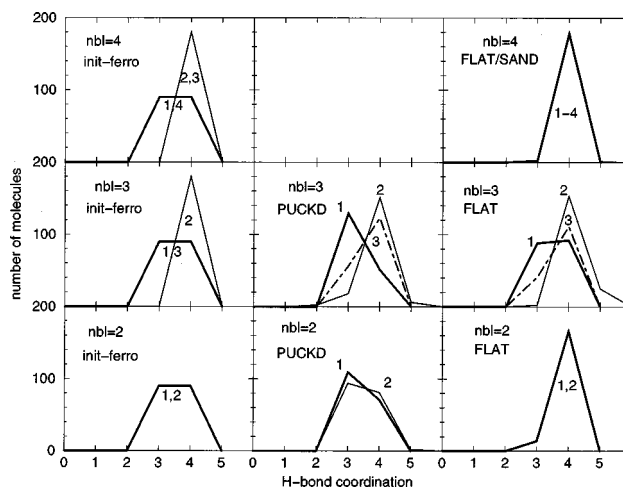


FIG. 3. Hydrogen bond coordination distribution in the bilayers of the different models; nbl denotes the number of bilayers in each model. The numbers on the plots pertain to the indices of the bilayers, the bottom rigid bilayer is numbered 1. The left-hand side plots are for the unrelaxed initial ferroelectric structures. The remaining results are for the end structures of the trajectories, before the recoiling.

III. RESULTS

A. The FLAT and SEMI models, two bilayers

In the FLAT model, the bottom bilayer is nearly flat, according to a structure given by Ref. 13 for a water bilayer on Ru (001). Relaxation of the initial ferroelectric structure by heating and recoiling had a dramatic restructuring effect

2 bi-layers, FLAT

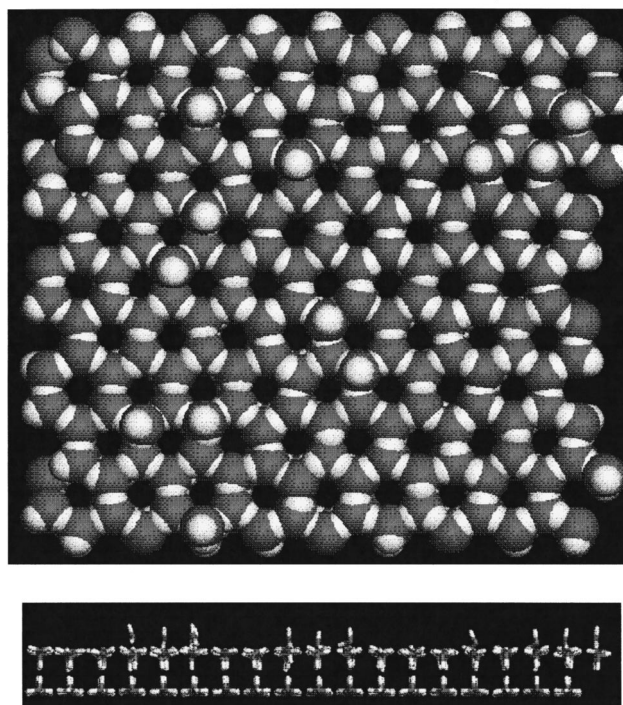


FIG. 4. A two bilayer FLAT model after a transition to a SANDWICH structure, top and side view. End structure of the trajectory before recoiling; the initial structure was ferroelectric. Note that the “up” and “down” OH bonds in the bottom figure do not point towards each other, but are laterally displaced, pointing towards the opposite O atoms.

3 bi-layers, FLAT

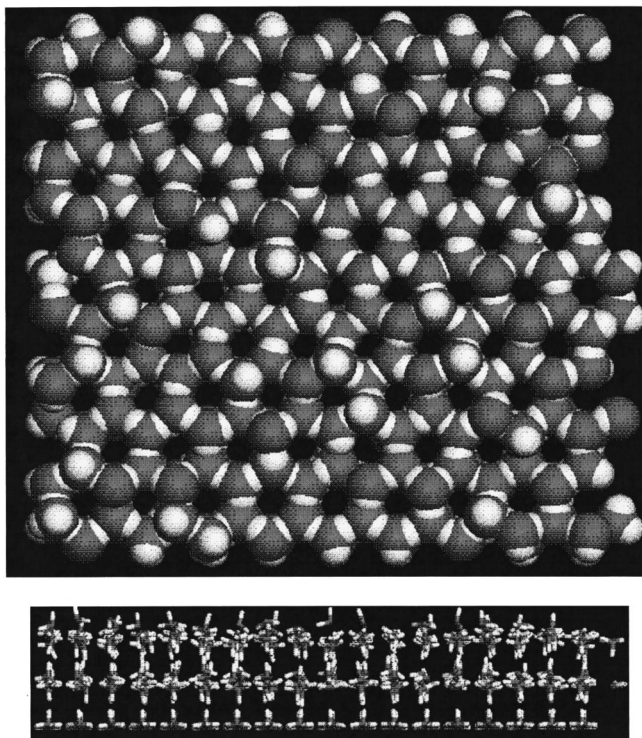


FIG. 5. A three bilayer FLAT model, after relaxation, top and side view. End structure of the trajectory, before recoling; the initial structure was ferroelectric. Note that the “up” and “down” OH bonds in the bottom figure do not point towards each other, but are laterally displaced, pointing towards the opposite O atoms.

(see Figs. 1–4). The entire top layer of dangling OH flipped, and most of the dangling-H atoms disappeared from the surface (compare Fig. 1 to Fig. 4). The dangling OH bonds “dived” into the surface and formed hydrogen bonds with water molecules directly below them. Thus, the number of hydrogen bonds between the two bilayers doubled. A large majority of water molecules became 4-coordinated. This type of structure has not been known until now (as far as we know) and is denoted below SANDWICH. The structural change to a SANDWICH occurs in early stages of the heating protocol. Note that the lateral arrangement of the O atoms does not change substantially during this rather dramatic rearrangement of the hydrogen bond network.

To strengthen the claim that the SANDWICH structure is the ground state of the system, we repeated the simulation starting from this structure; it remained stable during the entire relaxation cycle, and the final energy was slightly lower than that of a simulation starting from the ferroelectric initial conditions (see Table I). Note that the total z component of the SANDWICH dipole M_z is not zero but slightly positive, because of the assumed perfect rigidity of the bottom bilayer, versus thermal disorder in the upper bilayer. Also note that the “up” and “down” OH bonds in the bottom part of Fig. 4 do not face each other, but are laterally displaced, facing the opposite O atoms.

The structural transition to the SANDWICH is aided by the flatness of the bottom bilayer, since the flipped OH bond from the top bilayer has an O atom directly below it, at about

the “right” distance for strong hydrogen bonding. A similar conversion to a SANDWICH structure occurred for the SEMI (semiflat) model, in which the vertical spacing between the O atoms in the two halves of the bottom bilayer was set to 0.5 Å; the transition was associated with flattening of the top bilayer.

B. The FLAT model, three and four bilayers

As seen in Figs. 5 and 6, the surface dangling-H atoms “dived” again into the ice adsorbate layer to form additional H bonds. The resulting SANDWICH structure in the three bilayer model (Fig. 5) is a triple decker, with three bilayers interconnected by H bonds made by OH that point either up or down. The mean dipole $\bar{\mu}_z$ of the middle bilayer is positive but close to zero, the dipole of the top third bilayer is negative (see Fig. 2).

The four bilayer result is quite striking. The simulation resulted in two SANDWICHes on the top of each other, with almost no hydrogen bonds left between the second and the third bilayer! Moreover the two sandwiches are laterally displaced with respect to each other, as shown in Fig. 6 (the shift makes physical sense, since in an unshifted double sandwich structure, nonbonded O atoms of the second and the third bilayer would face each other). To strengthen the notion that this is the ground state, the relaxation cycle was

4 bi-layers, FLAT

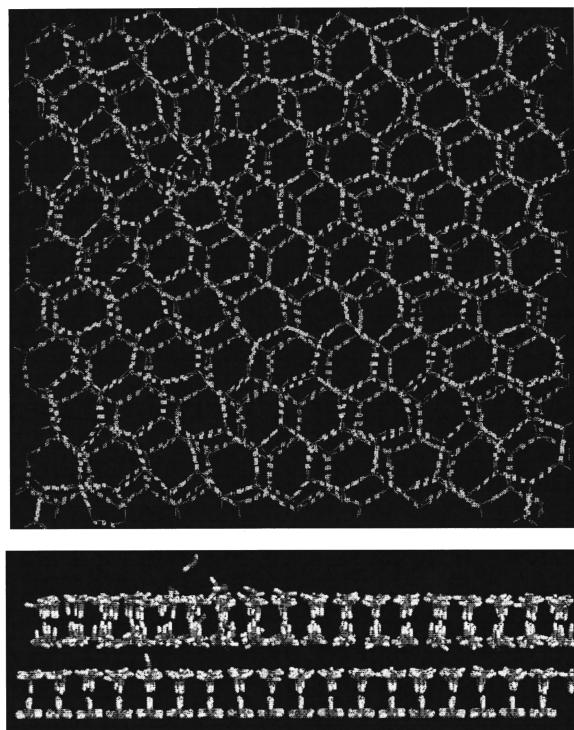


FIG. 6. A four bilayer FLAT model, top and side view, after the trajectory, before recoling. The initial structure was a double SANDWICH. A line model is used for the top view, to emphasize the shift between the top and the bottom SANDWICH. Note, that the “up” and “down” OH bonds in the bottom figure do not point towards each other, but are laterally displaced, pointing towards the opposite O atoms.

2 bi-layers, PUCKERED

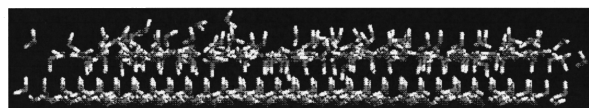
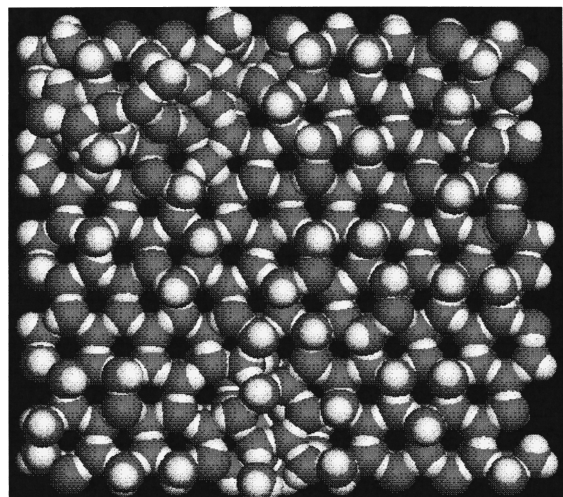


FIG. 7. A two bilayer PUCKERED model, top and side view, after the 190 ps trajectory, before recooling. The initial structure was ferroelectric (Fig. 1).

repeated starting directly from the double SANDWICH structure. The structure survived the entire relaxation cycle. The binding energy between the two sandwiches was estimated as only ~ 0.2 kcal/mol/molecule, by displacing the upper sandwich rigidly with respect to the lower one.

There is evidence for alternation of properties between even and odd numbers of bilayers in the FLAT model. The energy of the final configurations for the two, three, and four bilayer models is -10.8 , -11.0 , and -11.6 kcal/mol/molecule, respectively, suggesting enhanced stability for even numbers. Moreover, the upper bilayers in the even-numbered models are nearly flat, while the two upper bilayers in the three bilayer model are split (the z distribution of the O atoms in the second and the third bilayer is doubly peaked).

C. The PUCKERED model, two and three bilayers

Here, flipping of the dangling OH into the surface is not expected to be as favorable energetically as in the FLAT case, since the distance to the O atom below the OH is larger by some ~ 2 Å than the ideal hydrogen bond distance. Still, the flipped OH can enjoy some attractive interaction with molecules within the ice, while the “bare” dangling OH, sticking out of the surface, cannot. Therefore, the SANDWICHing effect still occurs, although not as dramatically as in the FLAT case. Still, the effect is large enough to reduce the bilayer dipole moment with respect to the “ideal” ferroelectric arrangement by more than a factor 5, over the thickness of only two or three bilayers (see Figs. 2, 7, and 8). Relaxation is also associated with some loss of order in the O arrangement, in accord with previous suggestions.^{11,12}

3 bi-layers, PUCKERED

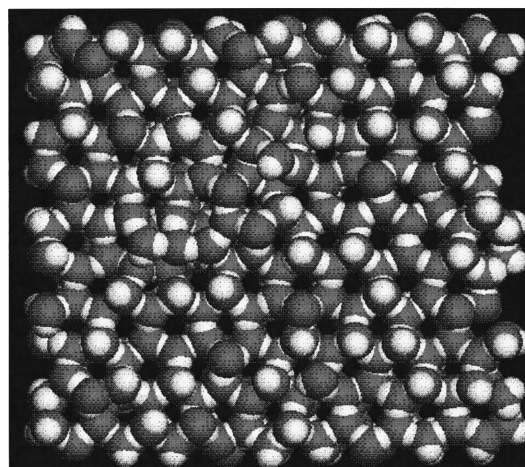


FIG. 8. A three bilayer PUCKERED model, top and side view, after the 178 ps trajectory, before recooling. The initial structure was ferroelectric.

From the present initial limited time simulations we cannot ascertain the exact extent of dangling-OH flipping, however, the results strongly suggest that substantial flipping does in fact occur. First, two 32 K simulations were carried out for two bilayers, starting from a fully ferroelectric and a fully SANDWICHed structure (see Table I). At this temperature, at which relaxation is impaired on the simulation time scale, the calculation starting from a SANDWICH resulted in a lower final energy than the one starting from the ferroelectric structure. Additional simulations were carried out, while heating the structures to 100 K, running a trajectory to allow for relaxation, and recooling. The lowest energy final structure was obtained in the longest (190 ps) simulation, starting from the ferroelectric structure (see Table I); in the course of this simulation only 36 “bare” dangling OH remained on the top surface, out of the initial number of 90 (compare Fig. 7 to Fig. 1). Similarly, in a 178 ps simulation of three bilayers, starting from a ferroelectric structure, the number of bare dangling OH sticking from the top bilayer was reduced from 90 to 42 (see Fig. 8). One may note that in the three bilayer systems, the internal dangling-OH wander all the way down to the bottom bilayer (see Fig. 8). Presumably, that occurs since in the present model the bottom bilayer molecules do not relax, and therefore make less favorable hydrogen bonds (which are easier to break) than those of H₂O in upper bilayers.

Note that the total number of dangling OH in the two systems did not decrease, and even increased slightly (see Table I), but most of them are internal dangling OH. These internal dangling OH represent a new type of defects in the ice structure, which allow for a rapid loss of ferroelectricity in ice adsorbate layers on metals.

D. The total dipole of the ice adsorbate layer, in the different models

The total dipole M_z is of interest since it is proportional to the contribution of the water dipole to the work function. The value of M_z for a single bilayer of an ideal ferroelectric structure is 0.94 D (the polarization of H_2O by the metal is not included in this value). The values of M_z obtained in the longest simulations for two and three PUCKERED layers are 1.17 and 1.67 D, respectively (these values may be still too large due to incomplete relaxation during the trajectory). The respective M_z values for the FLAT model, for one to four bilayers, are 0.56, 0.40, 0.54, and 0.47 D. The relatively modest change of M_z with the number of bilayers is qualitatively consistent with the experimentally measured modest variation of the work function as a function of number of ice bilayers on metals, after the first bilayer.^{5,9,18}

IV. SUMMARY

Simulations are presented of ice multilayers on metals. In the present (initial) model, the metal-ice interaction was not treated explicitly. Rather, the first bilayer structure was constructed based on suggestions in the literature, and set rigid. The simulations addressed the structure assumed by the subsequent bilayers, for a given bottom bilayer model. Two models were used. In one of them (denoted PUCKERED), perfect ice Ih (0001) structure was adopted for the O atoms in the bottom bilayer, with all OH bonds along the c axis pointing up. This structure is commonly assumed for ice bilayers on metals. In the second model (denoted FLAT), the bottom bilayer is assumed flattened by the interaction with the metal; the coordinates were adopted from the LEED study¹³ of an ice bilayer on Ru (001). The classical trajectory simulation cycle of the upper bilayers included heating to ~ 110 K, a trajectory near 110 K, and recooling to a temperature near 10 K.

Two issues were addressed. The first is the range and the mechanism of decay of ferroelectricity along the c axis. Polarization along the c axis is imposed by the metal on the first bilayer; and in a defectless ice structure it should propagate forever to the upper bilayers. However, the result would be an upper surface covered by a layer of repulsing dipoles (dangling OH); moreover very large values would be expected for the work function of a metal surface covered by completely polarized ice multilayers, contrary to experiment.^{5,9,18}

In simulated relaxed ice bilayers, ferroelectricity in fact decays fast. In the two bilayer and three bilayer PUCKERED models, the dipole of the top bilayer is reduced by a factor of nearly 6 with respect to the first bilayer (see Fig. 2). The ferroelectricity decay is associated with formation of a new form of defect in the ice structure, which (as far we know) has not yet been discussed in the literature. The defect can be described as "an internal dangling OH bond," and is formed when a dangling OH bond (that initially sticks out of the surface) "dives" into the surface, and points into a cavity below it. In the PUCKERED model, the O atom in the next bilayer, directly below such an OH, is much too far away for a formation of a good hydrogen bond. Still, the energy gain

from a conversion of a surface dangling OH to an internal dangling OH is sufficient to drive the formation of such defects, resulting in disappearance of a substantial fraction of dangling OH from the surface, and rapid decay of ferroelectricity. In the three bilayer PUCKERED model, the defects travel all the way to the bottom bilayer.

The second issue addressed pertains to the effect of the first bilayer flattening on the multilayer structure. The interaction with the metal is expected to flatten the first bilayer at least to some extent. In an unperturbed ice bilayer, the vertical distance between O atoms in the top and bottom layer is nearly 1 Å; and therefore only half of the molecules in neighboring bilayers are within a hydrogen bond distance from each other. The flattening brings *all* the water molecules in neighboring bilayers within a hydrogen bond distance. The effect on the adsorbate bonding structure is quite dramatic. In the FLAT model, ice multilayers adopt sandwich structures, which take advantage of the new bonding possibilities; concurrently, the majority of the dangling OH disappear from the upper surface. A two bilayer system adopts a single sandwich structure, in which the number of hydrogen bonds between the bilayers is doubled with respect to ordinary ice. A three bilayer system is a triple decker of three interconnected bilayers, while four bilayers assume a double sandwich structure, with two sandwiches shifted with respect to each other, and held together by a weak attractive interaction.

Further studies, including more elaborate treatment of the metal- H_2O interaction, are of course needed to verify these initial results.

ACKNOWLEDGMENTS

V.B. acknowledges gratefully the support of the ISF Grant No. 265/931. Helpful discussions are acknowledged with J. P. Devlin, G. Somorjai, J. Cowin, M. Asscher, S. Sibener, and P. Toennies.

- ¹N. Materer, U. Starke, A. Barbieri, M. A. van Hove, G. A. Somorjai, H. J. Kroes, and C. Minot, *J. Phys. Chem.* **99**, 6267 (1995).
- ²X. Su, L. Lianos, Y. R. Shen, and G. A. Somorjai, *Phys. Rev. Lett.* **80**, 1533 (1998).
- ³J. Braun, A. Glebov, A. P. Graham, A. Menzel, and J. P. Toennies, *Phys. Rev. Lett.* **80**, 2638 (1998).
- ⁴K. D. Gibson, M. Viste, E. Sanches, and S. J. Sibener, *Abstracts of ACS Papers* **215**: 035-Phys., Part 2, 2 April 1998.
- ⁵M. J. Idema, M. J. Dressler, D. L. Doering, J. B. Rowland, W. P. Hess, A. A. Tsekouras, and J. P. Cowin, *J. Phys. Chem. B* **102**, 9203 (1998).
- ⁶M. T. Sieger, W. C. Simpson, and T. M. Orlando, *Phys. Rev. B* **56**, 4925 (1997).
- ⁷F. E. Livingston, G. C. Whipple, and S. M. George, *J. Phys. Chem.* **101**, 6127 (1997).
- ⁸R. S. Smith, C. Huang, and B. D. Kay, *J. Phys. Chem.* **101**, 6123 (1997).
- ⁹T. Livneh, L. Romm, and M. Asscher, *Surf. Sci.* **351**, 250 (1996).
- ¹⁰P. V. Hobbs, *Ice Physics* (Clarendon, Oxford, 1974).
- ¹¹G. J. Kroes, *Surf. Sci.* **275**, 365 (1992).
- ¹²V. Buch, L. Delzeit, C. Blackledge, and J. P. Devlin, *J. Phys. Chem.* **100**, 10076 (1996); J. P. Devlin and V. Buch, *ibid.* **101**, 6095 (1997).
- ¹³G. Held and D. Menzel, *Surf. Sci.* **316**, 92 (1994).
- ¹⁴M. Morgenstern, J. Mueller, T. Michely, and G. Comsa, *Z. Phys. Chem.* **198**, 43 (1997).
- ¹⁵D. L. Doering and T. E. Madey, *Surf. Sci.* **123**, 305 (1982).
- ¹⁶S. Kawada, *J. Phys. Soc. Jpn.* **32**, 1442 (1972); Y. Tajima, T. Matsuo, and H. Suga, *Nature (London)* **299**, 810 (1982).
- ¹⁷(a) S. M. Jackson, V. M. Nield, R. W. Whitworth, M. Oguro, and C. C.

- Wilson, *J. Phys. Chem. B* **101**, 6142 (1997); (b) C. M. B. Line and R. W. Whitworth, *J. Chem. Phys.* **104**, 10008 (1996).
- ¹⁸(a) E. Langenbach, A. Spitzer, and H. Luth, *Surf. Sci.* **147**, 179 (1984); (b) M. Kiskinova, G. Pirug, and H. P. Bonzel, *ibid.* **150**, 319 (1985); (c) N. Kizhakevariam, X. Jiang, and M. J. Weaver, *J. Chem. Phys.* **100**, 6750 (1994); (d) N. Kizhakevariam, I. Villegas, and M. J. Weaver, *Surf. Sci.* **336**, 37 (1995). We believe that the number of bilayers in Fig. 9 of Ref. (d) should be divided by 2, following arguments of (a), based on infrared spectroscopy.
- ¹⁹(a) V. Buch, P. Sandler, and J. Sadlej, *J. Phys. Chem.* **102**, 8641 (1998); (b) U. Buck, I. Ettischer, M. Melzer, V. Buch, and J. Sadlej, *Phys. Rev. Lett.* **80**, 2578 (1998).
- ²⁰W. L. Jorgensen, J. Chandrasekhar, J. D. Madura, R. W. Impey, and M. L. Klein, *J. Chem. Phys.* **79**, 926 (1983).
- ²¹X. Xia, L. Perera, U. Essman, and M. L. Berkowitz, *Surf. Sci.* **335**, 401 (1995); X. Xia and M. L. Berkowitz, *Phys. Rev. Lett.* **74**, 3193 (1995).
- ²²E. Spohr, *J. Chem. Phys.* **107**, 6342 (1997).
- ²³S. Kuwajima and A. Warshel, *J. Phys. Chem.* **94**, 460 (1990).
- ²⁴J. A. McCammon and S. C. Harvey, *Dynamics of Proteins and Nucleic Acids* (Cambridge University Press, Cambridge, 1987).
- ²⁵(a) M. P. Allen and D. J. Tildesley, *Computer Simulations of Liquids* (Clarendon, Oxford, 1987), Chap. 5; (b) J. P. Valleau and S. G. Whittington, in *Statistical Mechanics A: Modern Theoretical Chemistry*, edited by B. J. Berne (Plenum, New York, 1977), Vol. 5, pp. 137–168; (c) C. Kittel, *Introduction to Solid State Physics* (Wiley, New York, 1971), Chaps. 13 and 14.
- ²⁶V. Buch, L. Delzeit, C. Blackledge, and J. P. Devlin, *J. Phys. Chem.* **100**, 10076 (1996).